Journal of Korean Magnetics Society, Volume 5, Number 5, October 1995

THE EFFECT OF HfB_2 ON MAGNETIC PROPERTIES OF NANOCOMPOSITE $Fe_2Nd_{14}B/Fe_3B$ MAGNET

ChoongJin Yang, ChanWook Kim and EyunByung Park

Electromagnetic Materials Laboratory, Research Institute of Industrial Science & Technology(RIST), P.O.Box 135, 790-600 Pohang, Korea

Abstract-By adding 1wt.% HfB_2 into $Nd_{3\text{-}4}Fe_{77\text{-}78.5}B_{18.5}$ alloys, the grain growth of $Fe_3B/Nd_2Fe_{14}B$ composite phases during annealing was found to be hindered by 40-50%. It is proposed that the addition of HfB_2 leads to the formation of fine dispersoids of HfB_2 in the $Fe_3B/Nd_2Fe_{14}B$ composite magnet. The maximum energy product($(B.H)_{max}$) as well as intrinsic coercivity($_iH_c$) for the $Nd_3Fe_{78.5}B_{18.5}$ + 1wt.% HfB_2 alloy were enhanced by more than 25% ($(B.H)_{max}$=10 MGOe, $_iH_c$=2.5 kOe) due to the addition of HfB_2 while remanent magntization(B_r) was reduced slightly. It is deduced that the formation of fine dispersoids will also play a role of magnetic domain pinning.

I .INTRODUCTION

Composite materials of magnetically hard and soft particles are excellent candidates for high performance permanent magnets[1-3]. In composite magnets soft magnetic grains cause a high magnetization and hard magnetic grains induce a large coercivity provided that the particles are small and strongly coupled[4,5]. Recently some experimental studies reported a nanostructured two-phase magnets with soft magnetic phase embedded in hard magnetic phase[6-9]. These materials has been attracting much attention because it possess a high saturation magnetization with a moderate coercivity inducing an applicable energy product.

In this study, we have prepared two-phase magnet of $Nd_2Fe_{14}B/Fe_3B$ nanocomposite where the $Nd_2Fe_{14}B$ grains are embedded in Fe_3B grains. The grain size of Fe_3B phase was intended to be controlled by introducing fine dispersoids of HfB_2 for enhancing the coercivity of nanocomposite magnets.

II .EXPERIMENTAL

$Nd_3Fe_{78.5}B_{18.5}$, $Nd_3Fe_{77.5}HfB_{18.5}$ and $(Nd_3Fe_{78.5}B_{18.5})$+1wt.% HfB_2 ingots were prepared by arc melting the constituent elements in an argon atmosphere. 50-60g pieces of ingot were melt spun from a quartz tube having an orifice diameter of 1 mm. A wheel speed of 40 m/sec was used. The melt-spun ribbons were then heat the magnetic properties. X-ray diffraction of Cu K_α radiation was used to identify the phases present and microstructure and composition were checked by transmission electron microscopy(TEM). The hysteresis loops were measured in a vibrating sample magnetometer(VSM) with a maximum magnetic field of 19 kOe along the long sample pieces to minimize demagntization effects. Thermomagnetic behaviors of the ribbon samples were traced by a thermogravimetric analyzer(TGA).

III.RESULTS AND DISCUSSION

The as-spun ribbons of each composition were found to be completely amorphous(actually might be microcrystallites) by x-ray diffractometry as shown in Fig. 1. Magnetic properties of the melt-spun ribbons for those compositions commonly showed an extremely low coercivity value although higher than 190 emu/g in experimentally saturated magnetization was obtained. Large coercivities were observed after annealing the samples above the crystallization temperature of each composition. For determining the optimized annealing temperature crystallization temperature was measured by calorimetric studies. Fig. 2 shows the variation of magnetic properties as a function of annealing temperature for the ribbons of (a) $Nd_3Fe_{78.5}B_{18.5}$, (b) $Nd_3Fe_{77.5}HfB_{18.5}$ and (c) $Nd_3Fe_{78.5}B_{18.5}$ + 1wt.% HfB_2, respectively.

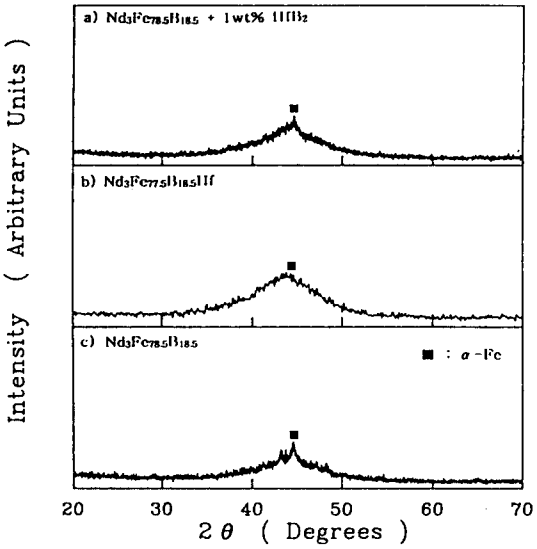

Fig.1 X-ray diffraction patterns of as-spun a) $Nd_3Fe_{78.5}B_{18.5}$ + 1wt% HfB_2, b) $Nd_3Fe_{77.5}B_{18.5}Hf$ and c) $Nd_3Fe_{78.5}B_{18.5}$ ribbons.

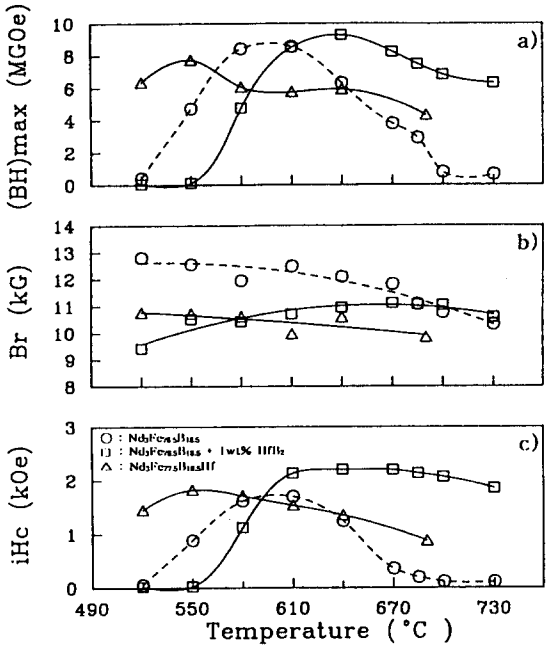

Fig. 2 Variation of magnetic properties of the melt-spun $Nd_3Fe_{78.5}B_{18.5}$, $Nd_3Fe_{77.5}B_{18.5}Hf$, and $Nd_3Fe_{78.5}B_{18.5}$ + 1wt% HfB_2 ribbons as a function of annealing temperature.

It is noteworthy that by adding Hf and HfB_2 into virgin $Nd_3Fe_{77.5}B_{18.5}$ composition, the maximum coercivity was measured to increase from 1.7 to 2.0 and 2.4 kOe, respectively. The annealing temperature at which the maximum coercivity was obtained also shifted to lower side(550 ℃) for $Nd_3Fe_{77.5}HfB_{18.5}$ with respect to $Nd_3Fe_{78.5}B_{18.5}$(610 ℃), while the maximum coercivity was obtained at a higher temperature(640 ℃) for $Nd_3Fe_{78.5}B_{18.5}$ + 1wt.% HfB_2 alloy. In accordance with the temperature giving the maximum coercivity values shown in figure(c), the maximum energy product was also measured in identical trend as shown in figure (a). Anyhow, the highest energy product of 10 MGOe was obtained after annealing at 640 ℃ for the alloy containing 1wt.% HfB_2. Owing to the addition of Hf and HfB_2 into $Nd_3Fe_{78.5}B_{18.5}$, however, deterioration in remanent magnetization was resulted as shown in figure (b). The remanence values were converted from measured data emu/g using the theoretical density(ρ =6.794 g/cm^3) of $Nd_3Fe_{78.5}B_{18.5}$ + 1wt.% HfB_2. After annealing the melt-spun ribbons of each composition between 520~730 ℃, x-ray diffraction patterns for the three different compositions commonly indicated that the composite magnetic alloys consist of Fe_3B and $Nd_2Fe_{14}B$ with a minor presence of α-Fe as shown in Fig. 3. The intensity distribution of $Nd_2Fe_{14}B$ and Fe_3B is the nature of isotropic powder sample. It can be seen in figures 3(a) and (b) that the addition of HfB_2 or Hf into $Nd_3Fe_{78.5}B_{18.5}$ may hinder the formation of α-Fe. That is evidenced by the weak intensity of (110) and (200) peaks compared with those in figure (c). In this regard the lower remanence values(B_r) for $Nd_3Fe_{78.5}B_{18.5}$ + 1wt.% HfB_2 and $Nd_3Fe_{77.5}B_{18.5}Hf$ alloys than those of $Nd_3Fe_{78.5}B_{18.5}$ in Fig. 2 can be explained. On the other hand, the variation of remanence values as a function of annealing temperature tends to be kept constant due to the addition of Hf or HfB_2.

Fig. 4 shows TEM micrographs showing the microstructure of melt-spun (a) $Nd_3Fe_{78.5}B_{18.5}$ and (b) $Nd_3Fe_{78.5}B_{18.5}$ + 1wt.% HfB_2 ribbons after heat treating at 760 ℃ for 30 min. The average grain size of matrix(Fe_3B) phase was measured to be less than 50 nm. By the addition of HfB_2, however, the average grain size was reduced to 30 nm. In order to indentify each Fe_3B, α-Fe and

Journal of Korean Magnetics Society, Volume 5, Number 5, October 1995

$Nd_2Fe_{14}B$ phase, selected area micro diffraction patterns were taken from the same sample shown in Fig. 4(b). Fig. 5(a) corresponds to the dark field image of α-Fe selected from the area shown in Fig. 4(a). Figure 5(b) demonstrates the uniformly distributed $Nd_2Fe_{14}B$ grains embedded in magnetically soft Fe_3B matrix grains. Fig. 5(c) and (d) illustrate the micro diffraction patterns taken from the selected dark field image of figure 5(a) and (b), respectively. Figures 5(c) and (d) indicating the [110] zone axis of α-Fe and [113] of $Nd_2Fe_{14}B$, respectively, give a strong confirmation that randomly distributed magnetically hard grains can be formed without any further growth during heat treatment. Fig. 5(a) indicates rather larger α-Fe grains compared with $Nd_2Fe_{14}B$ grains in figure 5(b). If the growth rate of α-Fe and $Nd_2Fe_{14}B$ grains is supposedly the same(actually should not be), figure 5(a) suggest that α-Fe forms ahead of the formation of $Nd_2Fe_{14}B$ phase. Fig. 6 shows thermomagnetic behaviors of melt spun $Nd_3Fe_{78.5}B_{18.5}$ + 1wt.% HfB_2 ribbons heat treated at the temperature as captions indicate. The ribbons heat treated at 550 ℃ for 30 minutes suggests the presence of Fe_3B for the main phase and α-Fe for the minor phase. However, one can see the hump shown about 320 ℃ suggesting that the formation of $Nd_2Fe_{14}B$ phase also took place during annealing at 550 ℃ though it might be neglegible. When the ribbons were annealed at higher temperatures such as 670 or 730 ℃, an active formation of $Nd_2Fe_{14}B$ and Fe_3B phases are suggested by the curves in which strong magnetic force are observed over the temperature range of 320~520 ℃. Curie temperature of Fe_3B phase in this study was measured to be 510 ℃ which is very close to that of Coehoorn et al.[10] observed(513 ℃). At the same time the curves suggest the further formation of α-Fe indicated by the rising hump shown around 700-740 ℃ as the annealing temperature increases.

In conclusion the enhanced remanent magnetization is attributed to the formation of fine dispersoids of HfB_2[11,12]. The formation HfB_2 on the order of 1000-2000 Å was reported

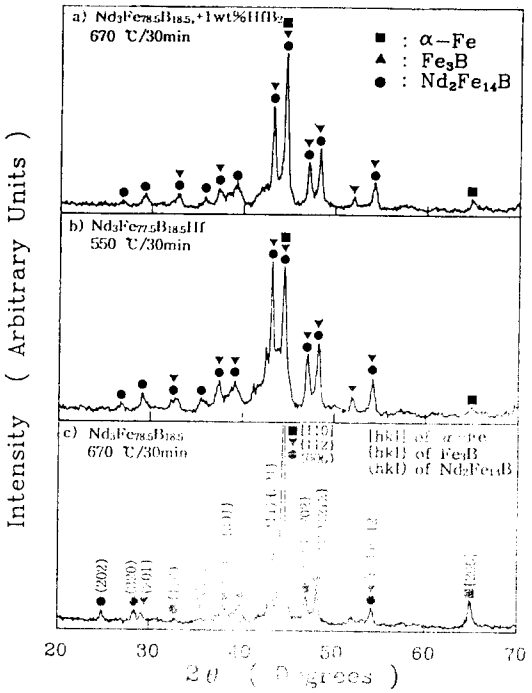

Fig. 3 X-ray diffraction patterns of melt-spun a) $Nd_3Fe_{78.5}B_{18.5}$ + 1wt% HfB_2, b) $Nd_3Fe_{77.5}B_{18.5}Hf$ and c) $Nd_3Fe_{78.5}B_{18.5}$ ribbons after heat treatment.

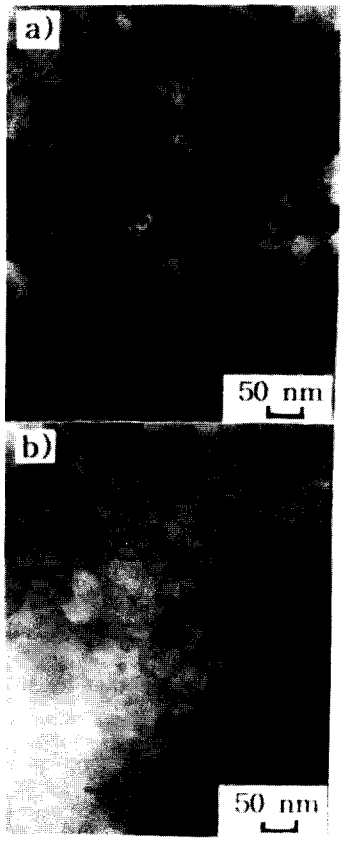

Fig. 4. TEM micrographs showing the microstructure in melt-spun (a)$Nd_3Fe_{78.5}B_{18.5}$ and (b)$Nd_3Fe_{78.5}B_{18.5}$+1 wt.%HfB_2 ribbons after heat treatment at 670℃ for 30 min.

to stabilize a fine grain structure of Nd-Fe-B based magnets.

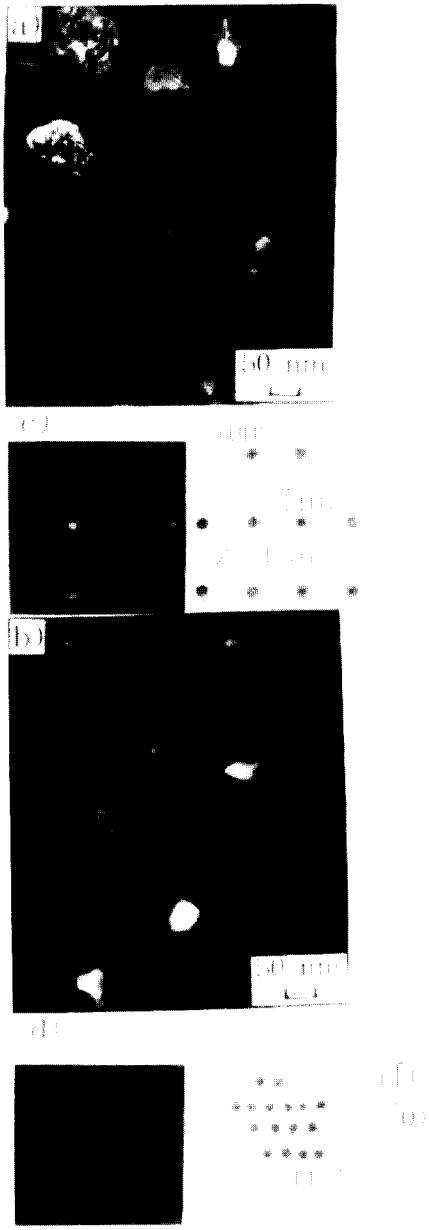

Fig. 5. TEM micrographs showing the grain aspect of melt-spun $Nd_3Fe_{78.5}B_{18.5}$+1wt.%HfB_2 ribbons after heat treatment at 670 ℃/30min. (a), (b) dark field images, and (c),(d) micro diffraction patterns showing α-Fe and $Nd_2Fe_{14}B$, respectively.

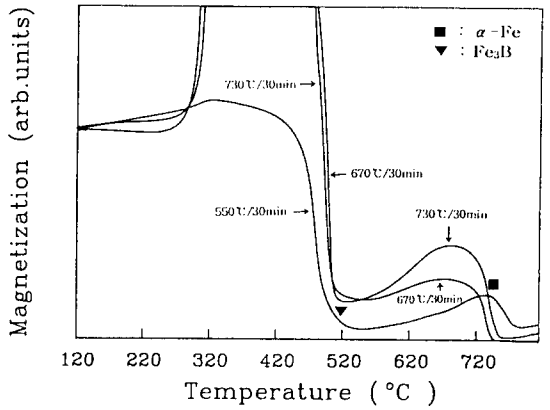

Fig.6.Thermomagnetic behaviors of melt-spun $Nd_3Fe_{78.5}B_{18.5}$ + 1wt% HfB_2 ribbons after hea treatment.

REFERENCES

[1] R.Skomsky and J.M.D.Coey, IEEE Trans. Magn. 30(2), 607(1993).

[2] T.Schrefl, R.Fisher, J.Fidler and H.Kronmuller, J. Appl. Phys. 76(10), 7053(1994).

[3] R.Skomsky, J. Appl. Phys. 76(10), 7059(1994).

[4] E.F.Kneller and R.Hawig, IEEE Trans. Magn. 27(4), 3588(1991).

[5] R.Skomsky and J.M.D.Coey, IEEE Trans. Magn. 29(6), 2860(1993).

[6] R.Coehoorn and C.de Waard, J. Magn. Mag. Mat. 83, 228(1990).

[7] A.Manaf, P.Z.Zhang, I.Ahmad and R.A. Buckley, IEEE Trans. Magn. 29(6), 866(1993).

[8] L.Withanawasam, G.C.Hadjipanayis and R.F. Krause, J. Appl. Phys. 75(10), 6646(1994).

[9] H.Kanekiyo, M.Uehara and S.Hirosawa, IEEE Trans. Magn. 29(6), 2863(1993).

[10] R.Coehoorn, D.B.de Mooij and C.de Waard, J. Magn. Mag. Mat. 80, 101(1989).

[11] C.J.Yang and R.Ray, J of Metals 41(9), 42(1989).

[12] B.G.Demczyk, Proc. of 11th Inter, Conference on Rare-Earth Magnets and Their Aplications, (Pittsburgh, PA, Carnegie Mellon University, Oct., 1990).